ELSEVIER

Earth and Planetary Science Letters 192 (2001) 439–446

EPSL

www.elsevier.com/locate/epsl

Magnetic properties of Kurokami pumices from Mt. Sakurajima, Japan

Yongjae Yu [a,*], David J. Dunlop [a], Özden Özdemir [a], Hiromoto Ueno [b]

[a] *Geophysics, Physics Department, University of Toronto at Mississauga, Room 3004, South Building, 3359 Mississauga Road North, Mississauga, ON, Canada L5L 1C6*

[b] *Department of Earth and Environmental Sciences, Kagoshima University, Kagoshima 890, Japan*

Received 31 March 2001; received in revised form 26 July 2001; accepted 26 July 2001

Abstract

Both chromite and low-Ti titanomagnetite are carriers of natural remanent magnetization (NRM) in Kurokami andesitic pumices of Mt. Sakurajima, Japan. Thermal demagnetization of the NRM and of a laboratory isothermal remanence indicate unblocking of chromite remanence between 200 and 260°C and of titanomagnetite remanence between 400 and 520°C. Electron microprobe analyses support the compositions $Fe_{1.9}Cr_{1.1}1O_4$ and $Fe_{2.9}Ti_{0.1}O_4$ indicated by the respective Curie temperatures of 260°C and 520–530°C. Chromite is thermally unstable and converts to magnetite during thermal demagnetization, leading to a self-reversal of NRM between 500 and 580°C. The chromite contributes about 25% of the NRM intensity of the sample.

Keywords: chromite; titanomagnetite; pumice; Sakura-jima; magnetic properties

1. Introduction

Chromites, members of the solid solution series $Fe^{2+}\ Cr^{3+}_{2-n}\ Fe^{3+}_{n}\ O_4$ with $0 \leq n \leq 2$, are common in submarine gabbros [1], in Precambrian sepentinite [2], in kimberlites [3], in volcanic rocks [4,5], in lunar rocks [6], and in Martian meteorites [7]. Coexistence of chromites and titanomagnetites has been reported in subaerially extruded olivine basalts and in island–arc volcanic rocks [4,5,8]. However, chromite has only rarely been reported as a carrier of natural remanent magnetization (NRM) with unblocking temperatures higher than room temperature [9]. Preliminary studies on Kurokami pumices from Mt. Sakurajima, Japan revealed several interesting magnetic properties that are difficult to explain in terms of titanomagnetite only [10]. The present study confirms that chromite is a carrier of NRM in Kurokami pumices.

Located in southernmost Kyushu, Sakurajima volcano consists of three main cones, Kitadake (1117 m), Minamidake (1040 m), and Nakadake (1060 m) as well as several small parasitic cones. Since A.D. 764, five historical major eruptions have taken place [11]. Nagasakibana lava erupted in A.D. 764–766. After a dormant period of 700 years, three large eruptions took place, Bummei lava (A.D. 1471–1476), An-ei lava (A.D. 1779),

* Corresponding author. Fax: +1-905-828-3717.
E-mail address: yjyu@physics.utoronto.ca (Y. Yu).

0012-821X/01/$ – see front matter
PII: S0012-821X(01)00464-2

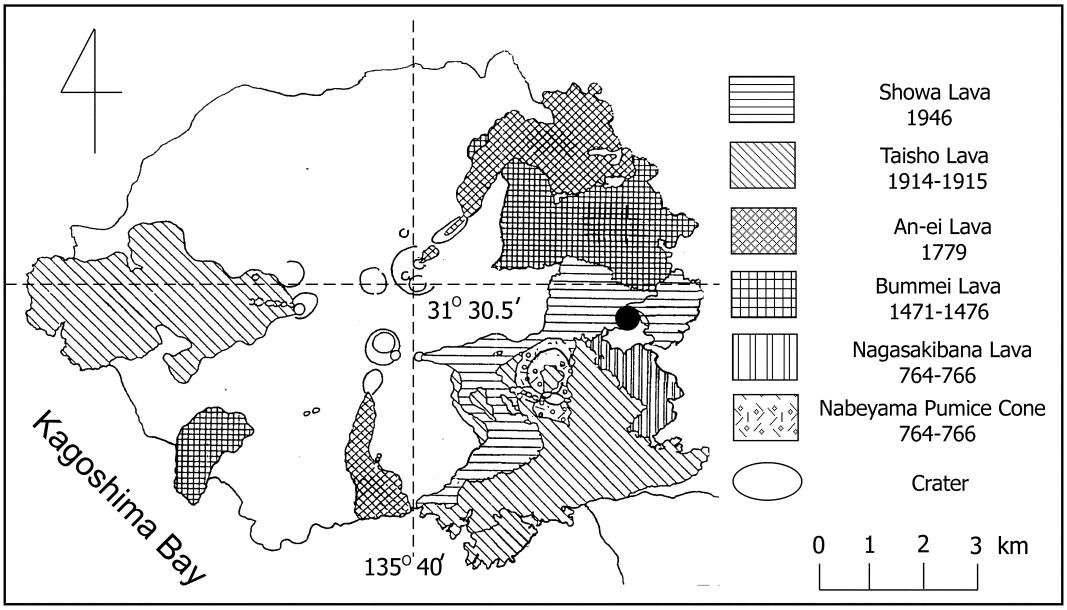

Fig. 1. A simplified geologic map showing the Kurokami sampling location (solid circle).

and Taisho lava (A.D. 1914). In 1939, small eruptions occurred at the parastic crater in the eastern slope near the summit of Minamidake. In 1946, Showa lava erupted with pyroclastic materials from the same parastic crater as the 1939 eruption [12]. The Showa lava has a flat surface of thick pumice deposits and is cut by deep valleys whose smooth bottoms consist of dark andesite and reddish welded pumice [13].

A simplified geologic map of Mt. Sakurajima is shown in Fig. 1. Four unoriented block samples were collected at Kurokami site (solid circle). Kurokami pumices are from the andesite formation of the Showa lava.

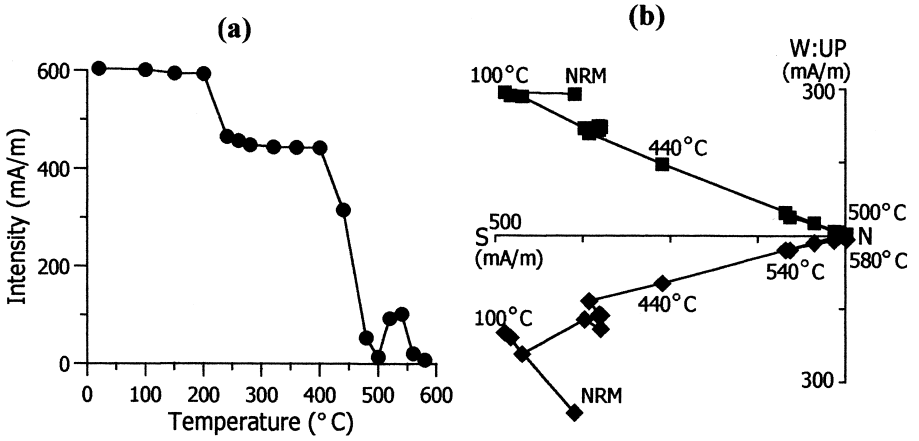

Fig. 2. An example of thermal demagnetization of NRM, showing the presence of phases A and B, with maximum unblocking temperatures of 240–260°C and ≈500°C, respectively, and a self-reversal of NRM (phase C, 500–580°C). (a) Total intensity decay of magnetization. (b) Vector projections: squares and diamonds are horizontal- and vertical-plane projections.

2. Magnetic properties

2.1. Thermal demagnetization of NRM

Three or more cylindrical specimens 23 mm in diameter and 21 mm in height were cut from each block sample. Thermal demagnetization was performed in 50°C steps to 500°C and then every 20°C up to 600°C using MMTD and Schonstedt furnaces. Fig. 2 shows typical thermal demagnetization results. Both lower unblocking temperatures of 200–260°C (phase A) and higher unblocking temperatures of 400–500°C (phase B) were observed (Fig. 2a). A partially self-reversed component (phase C) was also detected in the heating range between 500°C and 580°C. In vector projections, the phases A, B, and C show univectorial stability during thermal demagnetization (Fig. 2b). About one-quarter of the NRM is carried by the phase A.

2.2. Rock magnetic experiments

Thermal demagnetization of a composite isothermal remanence (Lowrie test, [14]) has been used to identify magnetic minerals. The isothermal remanence was acquired in fields of 1.2 T, 0.4 T, and 0.12 T applied successively along three orthogonal directions (z, y, and x). Thermal demagnetization of the soft (<0.12 T), medium (0.12–0.4 T), and hard coercivity (>1.2 T) components shows that phase B with unblocking temperatures of $\sim$520°C dominates all three components (Fig. 3). On the other hand, phase A is revealed by small decreases of remanence around 240–260°C for the hard and medium coercivity fractions.

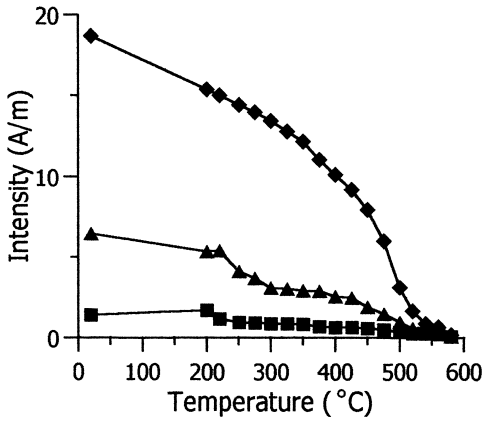

Fig. 3. Progressive thermal demagnetization of a composite isothermal remanence. The soft (diamonds), medium (triangles), and hard (squares) components were produced by applying sequential fields of 1.2 T, 0.4 T, and 0.12 T along z, y, and x axes, respectively.

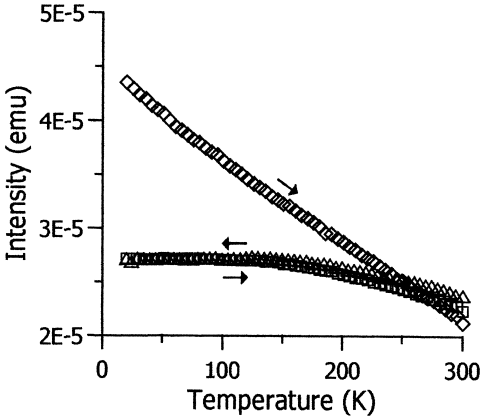

Fig. 4. Temperature dependence of low-temperature SIRM, produced by 2.5 T at 20 K, during zero-field warming to 300 K (diamonds), and zero-field cooling (triangles) and warming (squares) curves for an SIRM produced at 300 K in 2.5 T.

Low-temperature magnetic properties were measured on several rock chips using an MPMS2 SQUID magnetometer at the Institute for Rock Magnetism (IRM), University of Minnesota. First, saturation isothermal remanent magnetization (SIRM) was given by applying a field of 2.5 T at 20 K. Remanence was measured every 5 K during warming to 300 K in zero field (diamonds in Fig. 4). The result is a monotonic decrease of SIRM as the temperature increases. Another SIRM in 2.5 T was given at 300 K. The temperature dependence of this SIRM was determined every 5 K during cooling to 20 K (triangles) and then warming to 300 K (squares) in zero field. Almost reversible cooling and warming curves were obtained (Fig. 4).

In order to determine the Curie point of phase B, high-temperature thermomagnetic experiments were carried out for 17 individual grains using a Micro VSM at the IRM. The 17 octahedral grains, with diameters from 20 to 200μm, were

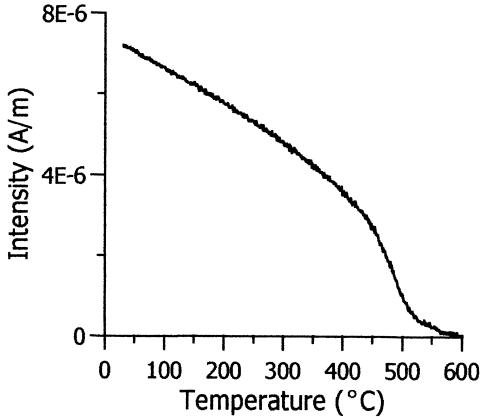

Fig. 5. High-field thermomagnetic curves for the individual titanomagnetite grains.

Table 1
Composition calculation based on electron microprobe analysis

Wt%	A1	A2	B	C
SiO_2	0.17	0.18	0.20	0.47
TiO_2	13.01	12.99	10.81	13.31
Al_2O_3	2.57	2.58	3.14	1.82
Cr_2O_3	0.04	0.04	0.04	0.00
FeO	41.59	40.87	39.15	41.65
Fe_2O_3	40.52	41.03	43.81	39.65
MnO	0.00	0.00	0.02	0.00
MgO	1.11	1.65	1.33	1.68
NiO	0.04	0.00	0.03	0.00
ZnO	0.00	0.00	0.03	0.00
CaO	0.00	0.01	0.00	0.00
Total	99.05	99.36	98.56	98.58

separated under the stereographic microscope using a hand magnet. Saturation magnetization was measured every 1°C from 20°C to 600°C in a 1-T field, yielding a Curie point for phase B of $\approx$530°C (Fig. 5), characteristic of titanomagnetite with $x \approx 0.1$ [15].

3. Magnetic mineral identification

To identify the magnetic phases, microscopic experiments were carried out using scanning electron microscopy (SEM) and electron microprobe. The composition of each grain was determined using two independent scanning electron microprobes, a Cameco SX-50 in the Geology Department, University of Toronto and a Hitachi S-4500 in the Materials Engineering Department, University of Toronto. Calibrations were made using ilmenite (SX-50) and cobalt (S-4500) standards. Samples were probed for Al, Ca, Cr, Fe, Mg, Mn, Ni, O, Si, Ti, and Zn (Table 1).

SEM photos show typical rhombus-shaped titanomagnetite crystals (Fig. 6a). An energy dis-

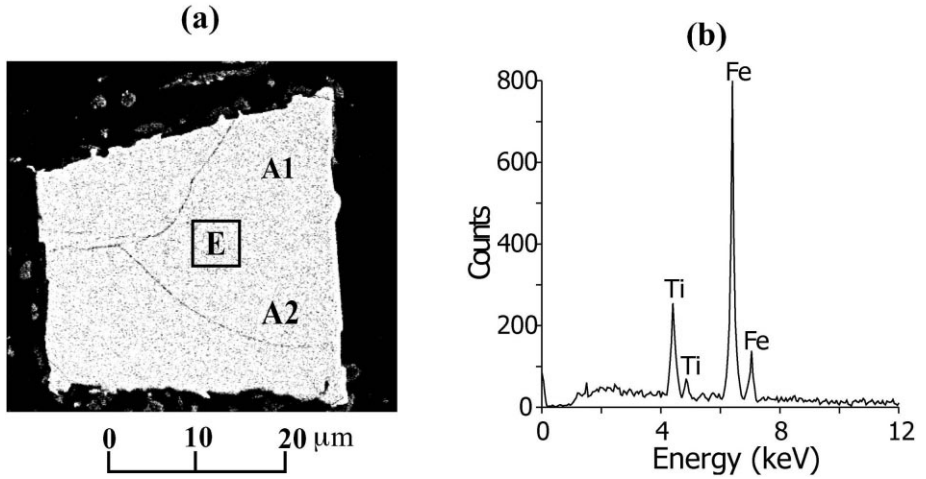

Fig. 6. (a) SEM image of a titanomagnetite grain (bright contrast). The microprobe analyses in Table 1 were carried out at A1 and A2 in (a) and on two other grains (B and C). (b) EDS from area E in (a).

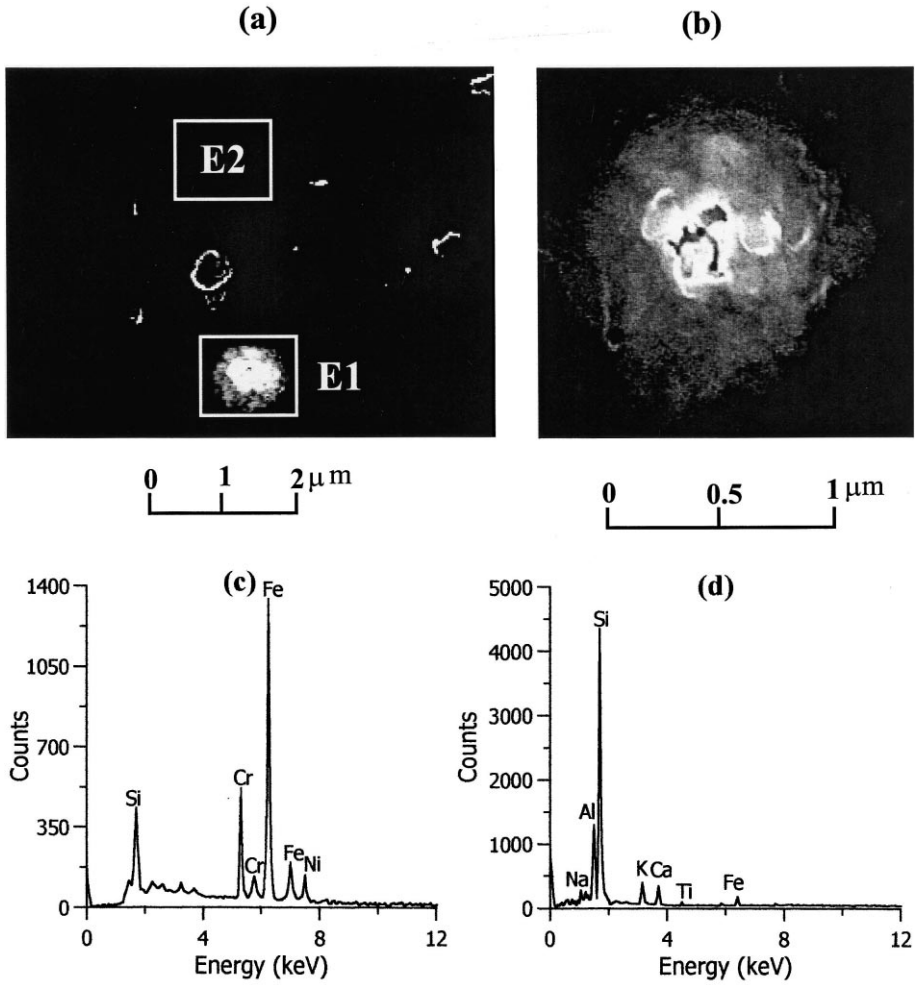

Fig. 7. (a) SEM image of a chromite grain. (b) Magnified image of the same chromite grain. (c) EDS from area E1 in (a). (d) EDS from area E2 in (a).

persive spectrum (EDS) from area E in Fig. 6a shows that Fe and Ti are the major cations (Fig. 6b). The EDS analyses normally counted numbers of ions for 1 min.

Quantitative microprobe analyses show on average 81–83 wt% of Fe, 11–13 wt% of Ti, and 3–4 wt% of other elements, mainly Al and Mg (Table 1). The analyses indicate that phase B is a low-Ti titanomagnetite with composition $x = 0.11$–0.13.

An example of an SEM image of another magnetic mineral (phase A) is shown in Fig. 7a. The image of the grain in Fig. 7ais magnified in Fig. 7b. Unfortunately, quantitative compositional analyses failed because the largest grain size of phase A was < 2 μm, smaller than the beam width. EDS from area E1 in Fig. 7a revealed four major elements, Cr, Fe, Ni, and Si (Fig. 7c), indicating that phase A is a Cr–Fe oxide (chromite) with Ni as a minor element. Microscopy (Fig. 7) suggests that the high coercivity of phase A in Fig. 3 results from its small grain size.

EDS obtained from the matrix (area E2 in Fig. 7a) indicate that Si is the dominant element in the matrix (Fig. 7d). For the EDS collected from the matrix, numbers of ions were counted for 10 min.

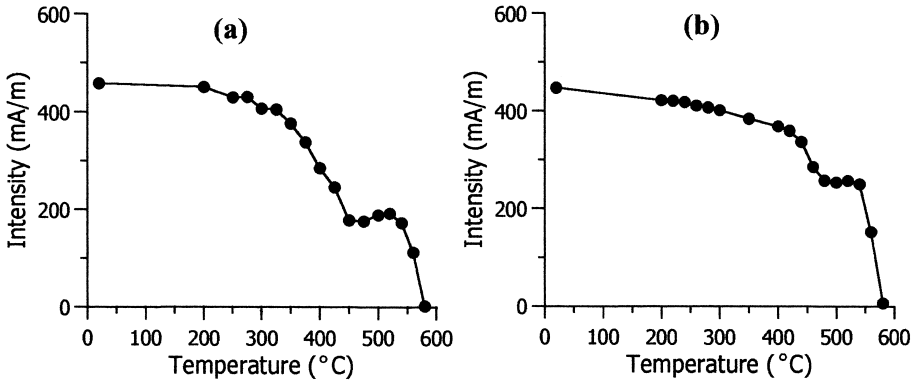

Fig. 8. (a) Stepwise thermal demagnetization of laboratory-produced TRM. TRM was produced in a field of 40 μT during cooling from 590°C. (b) Stepwise thermal demagnetization of a second TRM produced as in (a).

4. Thermal stability of chromite

Thermal stability of a laboratory-produced remanence was tested. After thermal demagnetization of the NRM, thermoremanent magnetization (TRM) was produced by cooling from 590°C in a laboratory field $H_{lab} = 40 \pm 0.2$ μT along the cylindrical axis of the specimens. Then progressive thermal demagnetization was carried out in similar thermal steps to those described in Section 2.1. After TRM was produced, phase B (titanomagnetite) recovered most of its original intensity (Figs. 2 and 8a). However, the signal of phase A (chromite) was low, with only a slight indication of remanence unblocking around 260°C (Fig. 8a). It is also interesting that the partially self-reversed phase C in Fig. 2abecame normally magnetized, with maximum unblocking temperatures of 580°C, indicating magnetite. Since there is little change of total intensity of phase B (titanomagnetite), oxidation of chromite (phase A) to magnetite (phase C) seems to be responsible for the anomalous increase of NRM intensity in the heating range between 500°C and 580°C (Fig. 2). When TRM was produced a second time, this repeated heating and cooling totally destroyed phase A but had less effect on phase B (Fig. 8b).

5. Discussion

5.1. Magnetic properties

Thermal demagnetization results (Fig. 2b) revealed maximum unblocking temperatures of phase A of ≈260°C. According to Francombe [16], a Curie point of 260°C corresponds to a chromite composition n ≈0.9, i.e., $Fe^{2+}\ Cr^{2+}_{1.1}\ Fe^{3+}_{0.9}\ O_4$. Although EDS analyses cannot provide a precise quantitative composition, they do give general support for this estimate of n. Comparison of peak intensities in Fig. 7c implies approximately twice as much Fe as Cr.

Interesting low-temperature behavior of Kurokami pumices was anticipated because both low-Ti titanomagnetite and chromite may potentially show low-temperature transitions. However, Fig. 4 shows no low-temperature transitions. Sharp remanence transitions in SIRM warming curves have been reported for low-Ti titanomagnetites ($x < 0.4$) [17]. For phase B (titanomagnetite), elements such as Al and Mg (see Table 1) may provide an explanation for the lack of a Verwey transition [18]. The estimated composition of phase A (chromite), based on its Curie point, is $n \approx 0.9$. Chromites in the compositional range between $n = 0.1$ and $n = 0.9$ do not show a low-temperature transition even though chromite has low-temperature phase transitions in four other composition ranges [19].

5.2. Thermal stability of chromite and paleomagnetic implications

A thermal stability test shows that phase A (chromite) oxidized to magnetite as a result of heatings to 600°C (Fig. 8). Haggerty [8] proposed that high-temperature oxidation of chromite, at least for oceanic basalts, happens under extremely oxidizing conditions. However, surface oxidation of chromite, a gradual compositional change to magnetite caused by prolonged metamorphism, has been reported for serpentinites [2]. Furthermore, as demonstrated by Kumar and Bhalla [9], formation of magnetite during thermal demagnetization of chromite-bearing rocks is not uncommon.

The existence of an NRM-carrying chromite in nature seems to require certain conditions. First, enough Cr, comparable to the amount of Fe, must be available. Cr is a more common element in the upper mantle than in the crust. Second, a quench-cooled environment is required to preserve magnetic chromites. Simulated TRM experiments (Fig. 8) and the results of Kumar and Bhalla [9] indicate that chromites cannot survive repeated heatings. Long-term exposure to above-ambient temperatures in nature may also oxidize chromite to other minerals. These two requirements explain why NRM-carrying chromites are rare in nature.

Acknowledgements

We thank Daniel Schulze and Barbara Murck of the Geology Department, University of Toronto for valuable discussions and Mike Jackson of the Institute for Rock Magnetism for his help with the measurements. Funding for the IRM is provided by the Keck Foundation, the National Science Foundation, Earth Sciences Division, and the University of Minnesota. We thank Claudio Cermignani of the Geology Department, University of Toronto and Fred Neub of the Materials Engineering Department, University of Toronto for microprobe analyses. We thank Subir Banerjee and David Clark for helpful reviews. This research has been supported by the Natural Sciences and Engineering Research Council of Canada through Grant A7709 to D.J.D.*[RV]*

References

[1] D.J. Dunlop, M. Prévot, Magnetic properties and opaque mineralogy of drilled submarine intrusive rocks, Geophys. J. R. Astron. Soc. 69 (1982) 763–802.
[2] N.W. Bliss, W.H. MacLean, The paragenesis of zoned chromite from central Manitoba, Geochim. Cosmochim. Acta 39 (1975) 973–990.
[3] D.J. Schulze, Chromite macrocrysts from southern African kimberlites: mantle xenolith sources and post-diamond re-equlibration, Afr. Geosci. Rev. 3 (1996) 203–216.
[4] R.B. Stewart, R.C. Price, I.E.M. Smith, Evolution of high-K arc magma, Egmont volcano, Taranaki, New Zealand: evidence from mineral chemistry, J. Volcanol. Geotherm. Res. 74 (1996) 275–295.
[5] V. Bannister, P. Roeder, A. Poustovetov, Chromite in the Paricutin lava flows (1943–1952), J. Volcanol. Geotherm. Res. 87 (1998) 151–171.
[6] D.J. Dunlop, Ö. Özdemir, Rock Magnetism: Fundamentals and Frontiers, Cambridge University Press, New York, 1997, pp. 573.
[7] B.P. Weiss, J.L. Kirschvink, F.J. Baudenbacher, H. Vali, N.T. Peters, F.A. Macdonald, J.P. Wikswo, A low temperature transfer of ALH84001 from Mars to Earth, Science 290 (2000) 791–795.
[8] S.E. Haggerty, Associated mineral oxidation, in: A.E. Goresy, S.E. Haggerty, J.S. Huebner, D.H. Indsley, D. Rumble (Eds.), Oxide Minerals, Mineral. Soc. Am., 1976, pp. HG-74.
[9] A. Kumar, M.S. Bhalla, Sources of stable remanence in chromite ores, Geophys. Res. Lett. 11 (1984) 177–180.
[10] Y. Yu, D.J. Dunlop, Ö. Özdemir, Rock magnetic and paleomagnetic experiments on hemoilmenites and titanomagnetites in some self-reversing pumices from Japan (abstract), EOS 79 (1998) F237.
[11] T. Kobayashi, K. Ishihara, 2. Historic eruptions and recent activities, in: S. Aramaki, K. Kamo, M. Kamada (Eds.), Sakurajima volcano, Kagoshima prefectural government, Kagoshima, 1988, pp. 7–12.
[12] K. Ishihara, T. Takayama, Y. Tanaka, J. Hirabayashi, Lava flows at Sakurajima volcano of the historic lava flows (1), volume of the historic lava flows, Ann. Sisast. Prev. Res. Inst. Kyoto Univ. 24B-1 (1981) 1–10.
[13] T. Kobayashi, 3. Geology and petrology, in: S. Aramaki, K. Kamo, M. Kamada, Sakurajima Volcano (Ed.), Kagoshima Prefectural Government, Kagoshima, 1988, pp. 13–27.
[14] W. Lowrie, Identification of ferromagnetic minerals in a rock by coercivity and unblocking temperature properties, Geophys. Res. Lett. 17 (1990) 159–162.
[15] S. Akimoto, Magnetic properties of FeO-Fe_2O_3–TiO_2 sys-

tem as a basis of rock magnetism, J. Phys. Soc. Japan 17 (Suppl. B1) (1962) 706–710.
[16] M.H. Francombe, Lattice changes in spinel-type iron chromites, J. Phys. Chem. Solids 3 (1957) 37–43.
[17] B.M. Moskowitz, M. Jackson, C. Kissel, Low-temperature magnetic behavior of titanomagnetites, Earth Planet. Sci. Lett. 157 (1998) 141–149.
[18] Ö. Özdemir, D.J. Dunlop, B.M. Moskowitz, The effect of oxidation on the Verwey transition in magnetite, Geophys. Res. Lett. 20 (1993) 1671–1674.
[19] M. Robbins, G.K. Wertheim, R.C. Sherwood, D.N.E. Buchanan, Magnetic properties and site distributions in the system $FeCr_2O_4$–Fe_3O_4, J. Phys. Chem. Solids 32 (1971) 717–729.